

SLAC-PUB-6251  
SLAC/SSRL-0036  
JUNE 1993  
(SSRL-M)

# X-ray Absorption Spectroscopy of Cuprous-Thiolate Clusters in Proteins and Model Systems.

Ingrid J. Pickering<sup>1</sup>, Graham N. George<sup>1</sup>,  
Charles T. Dameron<sup>2</sup>, Boris Kurtz<sup>2</sup>, Dennis R. Winge<sup>2</sup>  
and Ian G. Dance<sup>3</sup>

1. *Stanford Linear Accelerator Center, Stanford Synchrotron Radiation Laboratory,  
Stanford University, Stanford, CA 94309*

2. *Departments of Medicine and Biochemistry, University of Utah Medical Center,  
Salt Lake City, UT 84132*

3. *School of Chemistry, University of New South Wales, Kensington, N.S.W. 2033, Australia.*

(Submitted to the Journal of the American Chemical Society)

---

Work supported in part by the Department of Energy, Office of Health and Environmental Research, and the Department of Energy under Contract DE-AC03-76SF00515

## Abstract

Cuprous-thiolate multinuclear clusters exist in a range of different biological molecules for which no structural information exists from X-ray crystallography. Spectroscopic tools such as X-ray absorption spectroscopy have provided the major structural insights into this family of biological molecules. Recent nuclear magnetic resonance data on silver substituted metallothionein, thought to be analogous with the copper proteins, have suggested the presence of digonal coordination [Narula, S. S.; Mehra, R. K.; Winge, D. R.; Armitage, I. M. *J. Am. Chem. Soc.* **1991**, *113*, 9354-9358]. In order to test this in the copper case, we have examined a series of structurally characterized cuprous-thiolate model compounds, containing different proportions of digonal and trigonal copper sites using copper K-edge X-ray absorption spectroscopy. The edge spectra, which have been previously used as a probe for the average copper coordination environment in proteins, show little variation between the models, indicating that these are not useful as a probe of coordination environment in the case of cuprous thiolate clusters (as opposed to isolated metal sites). We show that systematic trends in the average Cu-S bond length from EXAFS curve-fitting analysis can be used to obtain an estimate of the fraction of digonal and trigonal copper sites. This correlation is applied to a series of different proteins containing cuprous thiolate clusters which are found to contain significant fractions of digonal copper.

## Introduction

Proteins containing cuprous-thiolate multimetallic clusters form a family of biological molecules for which structural information from crystallography is lacking. Structural information has, however, been obtained from spectroscopic techniques such as X-ray absorption spectroscopy (XAS) [e.g. 1 and refs. therein]. Copper metallothioneins have been intensively studied, and can be considered to be prototypical cuprous-thiolate proteins [1]. Metallothioneins are small, cysteine-rich, polypeptides which bind metal ions such as copper and zinc. In copper metallothioneins, the cysteine thiolates bridge the cuprous ions to form a multimetallic cluster [2,3].

Cuprous-thiolate multimetallic cluster proteins have diverse functions in a variety of organisms. In yeasts, the function of metallothioneins is to buffer the cellular cytoplasm of copper ions in order to minimize copper-induced toxicity [4]. The fission yeast *Schizosaccharomyces pombe* does not contain metallothionein; a physiologically equivalent role is fulfilled by the formation of cuprous-thiolate multimetallic clusters coated with glutathione-related isopeptides [5]. A similar function of buffering intracellular metal levels has been postulated for metallothionein in animal cells, although direct roles remain to be established [6,7]. Some DNA-binding proteins also contain cuprous-thiolate multimetallic clusters [8-10]. Yeast regulate the production of metallothionein by responding to the levels of copper or silver present in the growth medium [6,8,11-14]. This is done at the level of DNA transcription by intracellular copper sensor protein molecules which stimulate the transcription of the metallothionein gene in the presence of copper ions [8,13,14]. In the case of the yeast *Saccharomyces cerevisiae*, the formation of a multimetallic cuprous-thiolate cluster in the copper sensor protein (known as the ACE1, or CUP2, transcription factor [8,13]) is required to activate the expression of metallothionein genes [8-10]. A closely homologous protein AMT1, identified in *Candida glabrata*, mediates the expression of a family of metallothionein genes in this yeast [11,15]. The activation of ACE1 and AMT1 is specific for Cu(I) and Ag(I) ions [8-10]. The oncogenic protein E7 from *Papilloma* virus is capable of forming a cuprous thiolate cluster, although it is not clear whether the physiological role is fulfilled by a copper or zinc substituted protein [16]. Perhaps most significantly, a deficiency in a metallothionein-like protein has recently been implicated as a possible cause of Alzheimers syndrome [17]. The role of the metal clusters in this novel protein is currently under study.

In all known cases, the copper ions are present as Cu(I) and the sulfur ligands are provided by cysteinyl sulfurs. Proteins and peptides containing cuprous-thiolate clusters are known to have an abundance of cysteine residues [1,5,6,8,18,19], with a common sequence motif being Cys—X—Cys or Cys—X—X—Cys in which X represents any other amino acid. The conserved cysteinyl residues are very likely the ligands of the copper multimetallic cluster. No complete structures are as yet available for copper-thiolate multimetallic clusters in proteins. Nevertheless, strong chemical precedence exists for multimetallic copper-thiolate species [20]. X-ray crystal structures of several synthetic cuprous-thiolate multimetallic clusters have been determined [20]. Different stoichiometries have been characterized, including  $\text{Cu}_3\text{S}_3$ ,  $\text{Cu}_4\text{S}_4$ ,  $\text{Cu}_4\text{S}_6$ ,  $\text{Cu}_5\text{S}_6$ ,  $\text{Cu}_5\text{S}_7$ ,  $\text{Cu}_6\text{S}_8$ ,  $\text{Cu}_8\text{S}_8$ ,  $\text{Cu}_8\text{S}_{12}$  and  $\text{Cu}_{12}\text{S}_{12}$  [20-30]. In all of these clusters the copper possesses a formal cuprous oxidation state. Analyses of the structural features of these clusters has lead to a number of generalizations. Thiolate ligands tend to maintain low coordination numbers of Cu(I), and both digonal and trigonal coordination stereochemistries are common, sometimes coexisting in one cluster. The thiolate ligands are predominantly doubly-bridging (*ie.* coordinated to two metals), and these thiolate bridges, rather than copper-copper bonds, are the principal cohesive force in the clusters.

A limited number of spectroscopic techniques are available which can provide structural information for multimetallic clusters. Two of these are X-ray absorption spectroscopy (XAS) and high resolution NMR. These provide complementary information; XAS can provide local structural information with very accurate interatomic distances, but somewhat poor estimates of coordination number and scatterer size (atomic number), whereas high resolution NMR can, in some cases, provide an entire structure, although bond distances are less accurately determined. Although both naturally abundant isotopes of copper ( $^{63}\text{Cu}$  and  $^{65}\text{Cu}$ ) are magnetic with  $I=3/2$  and similar magnetic moments, the presence of nuclear quadrupole effects makes NMR less useful for this element. Recently, heteronuclear ( $^1\text{H}$ - $^{109}\text{Ag}$ ) multiple quantum coherence NMR studies performed on silver metallothionein from *S. cerevisiae* established the connectivities of ten cysteinyl residues with seven bound  $^{109}\text{Ag(I)}$  ions [3]. Ag(I) is isoelectronic to Cu(I), and their metal-thiolate compounds and thiolate clusters show similar structural principles; silver metallothionein is likely to be isostructural with copper metallothionein. In the case of metallothionein there is good evidence that the silver and copper proteins are structurally very similar [3], although in general caution should be exercised in extrapolating structural information on silver proteins to copper proteins as Ag-S bonds are typically more than 0.2 Å

longer than Cu-S bonds. Narula *et al.* [3] questioned the original proposal from XAS of an  $\text{Cu}_8\text{S}_{12}$  cluster stoichiometry with trigonal Cu(I) coordination [2]. Based on the NMR results, a new model cluster  $\text{M}_7\text{S}_{10}$  (M=Cu or Ag) was proposed, in which two of the seven metal ions may exist in digonal coordination with the remainder in trigonal coordination [3].

The suggestion of possible digonal Ag(I) ions in yeast silver metallothionein by NMR has prompted us to re-evaluate the XAS data from proteins containing cuprous-thiolate clusters. The question addressed is whether XAS can detect mixed coordination complexes in multimetallic cuprous-thiolate complexes. In this report, we present XAS data on a series of synthetic cuprous-thiolate multimetallic clusters containing different proportions of digonal and trigonal copper, together with new data on a series of cuprous-thiolate proteins. Figure 1 shows the crystal structures of the copper-sulfur cluster cores of the three model compounds used in this study [21,23,25,26]. The trends observed from these models provide new insights into the copper coordination for the protein systems and are used in the interpretation of the XAS of a number of different copper-thiolate proteins.

## Materials and Methods

**Sample preparation.** The compounds *bis*-(tetramethylammonium)hexa( $\mu$ -benzenethiolato)-tetracuprate(I)  $(\text{Me}_4\text{N})_2[\text{Cu}_4(\text{SPh})_6]$  (or  $\text{Cu}_4\text{S}_6$ ) [21,23,31], *bis*-(tetramethylammonium)hepta( $\mu$ -benzenethiolato)-pentacuprate(I),  $(\text{Me}_4\text{N})_2[\text{Cu}_5(\text{SPh})_7]$  (or  $\text{Cu}_5\text{S}_7$ ) [26] and (tetraethylammonium)hexa( $\mu$ -*t*-butylthiolato)-pentacuprate(I)  $(\text{Et}_4\text{N})[\text{Cu}_5(\text{SBu}^t)_6]$  (or  $\text{Cu}_5\text{S}_6$ ) [25], were prepared and characterized as previously described. Samples for X-ray absorption spectroscopy were finely ground under anaerobic conditions, appropriately diluted with boron nitride and packed into aluminum holders of 1mm path length with thin mylar windows.

Yeast copper metallothionein from *S. cerevisiae* was isolated from cultures grown in the presence of 1mM  $\text{CuSO}_4$  as purified, as previously reported [19]. The N-terminal half ACE1 from *S. cerevisiae* was purified from a T7 *Escherichia coli* expression system as described previously [9]. Metal-free ACE1 was prepared and the fully reduced sample was used for Cu(I) reconstitution [9]. Cu(I) was titrated into ACE1 according to the published protocol [9], except that reduced glutathione was mixed with the metal-free ACE1 to a final concentra-

tion of 5 mM prior to addition of 6.8 mol eq. Cu(I). The Cu:protein stoichiometry was verified using atomic absorption spectrophotometry and amino acid analysis.

Cu(I)- $\gamma$ EC peptide complexes from *S. pombe* were isolated from cultures grown in the presence of 1mM CuSO<sub>4</sub> as described previously [5]. Ligands for the Cu(I) complexes are provided by the cysteinyl thiolates of glutathione-related isopeptides of general sequence ( $\gamma$ EC)<sub>n</sub>G where *n* typically varies from 2 to 4. The actual Mr of the complex is unknown, but the apparent Mr is consistent with an oligomeric structure Cu<sub>x</sub>[( $\gamma$ EC)<sub>n</sub>G]<sub>y</sub> containing a poly-metallic cluster. Synthetic (EC)<sub>n</sub>G peptides were synthesized by solid phase peptide synthesis with either  $\alpha$  peptide linkages (EC)<sub>2</sub>G or the isopeptide variant ( $\gamma$ EC)<sub>n</sub>G using an Applied Biosystems (ABI) 431A Peptide Synthesizer on *p*-hydroxymethylphenoxymethyl resin. The synthesis was carried out in the presence of 1-hydroxybenzotriazole and N,N-dicyclohexyl carbodiimide with N-FMOC-glycine (ABI), N-FMOC-L-cysteine-Trt (ABI), N-FMOC-L-glutamic acid- $\gamma$ -*t*-butyl ester (ABI), and N-FMOC-L-glutamic acid- $\alpha$ -*t*-butyl ester (Bachem) using N-methylpyrrolidone as the solvent. Peptides were cleaved from the resin and side chains de-blocked at room temperature with 95% TFA, 2.5% water and 2.5% ethanedithiol. After drying the cleavage products on a rotary evaporator, the samples were resuspended in 5% acetic acid and purified by preparative C<sub>18</sub> reverse phase HPLC in 0.1% TFA and a linear gradient of acetonitrile. The isolated peptides were quantified by amino acid analysis. The Cu(I) complexes with the synthetic peptides were formed with 1.5 mol eq. Cu(I) per peptide. No glutathione was included in the reconstitution. Samples for X-ray absorption spectroscopy were prepared with 15% glycerol, and frozen in lucite cuvettes with thin mylar windows. The final copper concentration was close to 3 mM.

CuE7 was prepared as described previously [16].

**XAS data collection and analysis.** Copper K-edge X-ray absorption spectra were collected on beamline SB07-3 (1.8T wiggler field) at the Stanford Synchrotron Radiation Laboratory, with the storage ring SPEAR operating at 3 GeV with ring currents of 50-100 mA. Si(220) monochromator crystals were used, with an upstream vertical aperture of 1 mm. X-ray absorption was monitored either by measuring the Cu K <sub>$\alpha$</sub>  fluorescence excitation spectrum using a Canberra 13-element Ge array detector [32], or by measuring the X-ray transmittance using nitrogen-filled ionization chambers. The former was used in the case of the protein samples, and the latter for the model compounds. Samples were held at a constant temperature in the

range 4-8 K using an Oxford Instruments CF1204 liquid helium flow cryostat. Energy calibration was carried out by simultaneously recording the spectrum of copper metal, assuming 8980.3 eV for the lowest energy K-edge inflection. The extended X-ray absorption fine structure (EXAFS) oscillations  $\chi(k)$  were quantitatively analyzed by a curve-fitting procedure [33] to the following approximate expression:

$$\chi(k) = \sum_{i=1}^n \frac{N_i A_i(k, R_i)}{k R_i^2} \exp\left(\frac{-2R_i}{\lambda(k, R_i)}\right) \exp\left(-2\sigma_i^2 k_i^2\right) \sin\left[2kR_i + \phi(k, R_i)\right] \quad (1)$$

Here  $k$  is the photoelectron wave number, and  $N_i$  is the number of  $i$ -type atoms at a mean distance  $R_i$  from the absorber atom (in this case copper). The summation is over all sets of equivalent atoms,  $n$ . The functions  $A(k, R_i)$ ,  $\lambda(k, R_i)$  and  $\phi(k, R_i)$  are the curved-wave total EXAFS amplitude, photoelectron mean free path, and total EXAFS phase functions, respectively. For the first shell Cu-S contacts, these were calculated in the single scattering approximation using the program *feff* (single scattering code, version 4) of Rehr and co-workers [34]. The value of  $\Delta E_0$ , a small correction to the energy for  $k = 0$  (routinely chosen at the arbitrary value of 9000 eV) was determined to be -12.3 eV from an initial refinement of the  $\text{Cu}_4\text{S}_6$  cluster data, and was held constant at this value for all other fits. For the Cu-Cu outer shells, the phase and amplitude functions were extracted from the  $\text{Cu}_4\text{S}_6$  cluster data in the following way. The Cu-S shell was fitted, and then a residual spectrum was calculated. The residual spectrum was Fourier transformed, and then the scatter peak due to the Cu-Cu shell was filtered, back-transformed and the phase and amplitudes extracted assuming  $N = 3$ ,  $R = 2.740 \text{ \AA}$  and  $\sigma^2 = 0.0075 \text{ \AA}^2$ .

## Results

*Cu K-edge XAS of synthetic Cu(I)-thiolate cluster model compounds.* Copper K-edge X-ray absorption edge spectra of the three synthetic Cu(I)-thiolate clusters of stoichiometries  $\text{Cu}_4\text{S}_6$ ,  $\text{Cu}_5\text{S}_7$  and  $\text{Cu}_5\text{S}_6$  are shown in Figure 2. Also included for comparison is the spectrum of  $\text{Cu}(\text{tmtu})_3\text{BF}_4$  [35], which contains an isolated Cu(I) atom in trigonal planar coordination by the uncharged ligand tetramethylthiourea (tmtu). As expected for formally Cu(I) complexes, none of the spectra show observable  $1s \rightarrow 3d$  transitions at about 8978 eV. The four spectra are quite similar, with a pronounced feature at about 8984 eV having only subtle differences in structure and intensity.

At first sight, this result seems at odds with the previous work of Kau *et al.* [36]. In a comprehensive study of Cu(I) and Cu(II) X-ray absorption edges, these workers [36] observed that the 8984 eV peak was a sensitive indicator of Cu(I) coordination, the peak being most intense for digonal and least intense for tetragonal copper coordination. This peak was assigned as the formally dipole-allowed  $1s \rightarrow 4p$  transition, and the data were rationalized from the expected degeneracy of the  $4p$  orbital from simple ligand field arguments [36]. The studies of Kau *et al.* [36], however, did not include digonal Cu(I) complexes with thiolate ligands, nor did these workers examine the spectra of cuprous-thiolate clusters with mixed digonal and trigonal copper coordination. The coordination of cuprous-thiolate species will have a greater covalency than nitrogen or oxygen coordination, and the corresponding filling of the Cu  $4p$ -orbitals would reduce the intensity of the 8984 eV peak. This provides a possible explanation of the lack of increased intensity of the 8984 eV peak for  $\text{Cu}_5\text{S}_7$  and  $\text{Cu}_5\text{S}_6$  with respect to  $\text{Cu}_4\text{S}_6$ . A further cause of reduction in intensity of this peak in the digonal case, which Kau *et al.* [36] investigated, is the T-shaped coordination in which another species interacts with the metal orthogonally to the two ligands. Although there is no structural evidence for unusually short interionic interactions in the model compound crystals [23,26,37], there is some evidence for intracluster interactions which could well affect the edge spectra. The digonal S-Cu(I)-S species all show a slight displacement of the copper towards the center of the cluster (angles S-Cu-S are  $175.2^\circ$  for  $\text{Cu}_5\text{S}_7$  and a mean of  $170.1^\circ$  for three angles in  $\text{Cu}_5\text{S}_6$ ). Similarly, there is local distortion of up to  $20^\circ$  in the S-Cu-S angles at some of the trigonal sites in all three compounds. For the digonal coppers in  $\text{Cu}_5\text{S}_6$  the closest Cu-Cu contacts are two trigonal coppers at about 2.7 Å, and two digonal coppers at about 3.2 Å. The presence of coppers at these distance may influence the unoccupied energy levels. The presence of Cu-Cu contacts for trigonal copper at around 2.7 Å suggests that Cu-Cu contacts may also be significant for the interpretation of the edge spectra in this case. Deviations from ideal planarity and linearity will also change unoccupied energy levels, causing splitting and hence reducing the apparent intensity of the transition. The deviation from the ideal geometry also causes greater mixing of Cu  $4s$ -orbitals with the Cu  $4p$ -orbitals, making the transition less allowed. Finally, the cuprous-thiolate clusters contain several occurrences of Cu(I), each in a crystallographically distinct environment, with corresponding subtle variation electronic structure. These small differences might cause the spectral features to become broadened (smeared out) and thus less intense. There are thus several possible causes for a lowering of the 8984 eV  $1s \rightarrow 4p$  transition intensity, and probably all have some effect.



In any case, setting theoretical arguments aside, it is clear from our results that the intensity of the 8984 eV transition in Cu K-edge spectra is not a good measure of the presence of digonal Cu(I) in copper(I)-thiolate cluster compounds. We therefore chose to investigate whether the Cu-S distance, which can be accurately determined from the EXAFS, could be used to determine digonal Cu(I).

*Cu K-edge EXAFS of synthetic cuprous-thiolate clusters.* The copper K-edge EXAFS spectra of  $\text{Cu}_4\text{S}_6$ ,  $\text{Cu}_5\text{S}_7$  and  $\text{Cu}_5\text{S}_6$  are shown in Figure 3A, together with the results of EXAFS curve fitting analysis, and the corresponding Fourier transforms in Figure 3B. The Fourier transforms all have two main peaks, indicating that the EXAFS is dominated by two prominent interactions. The transform peak at around 2.2 Å is due to the Cu-S interactions, while the peak at around 2.7 Å is predominantly due to Cu-Cu interactions. The Cu-Cu peak varies more in magnitude with the cluster composition than the Cu-S contact. For the  $\text{Cu}_5\text{S}_6$  EXAFS, trace contamination by zinc (Zn K-edge at around 9660eV, or  $k = 13.1 \text{ \AA}^{-1}$ ) caused truncation of the data at  $k = 13 \text{ \AA}^{-1}$ , compared with a maximum of  $15 \text{ \AA}^{-1}$  in the other two data sets. An even smaller trace of zinc in the  $\text{Cu}_5\text{S}_7$  sample manifests itself in the small feature at around  $13.1 \text{ \AA}^{-1}$ , but this does not adversely affect the fitting in this case.

As noted above,  $\text{Cu}_5\text{S}_7$  and  $\text{Cu}_5\text{S}_6$  contain both trigonal and digonal copper. The crystal structures of all three models [21,23,25,26] (Figure 1) indicate an average trigonal Cu-S bond distance of 2.28 Å and an average digonal Cu-S bond distance of 2.16 Å. Thus, the Cu-S bond-length is around 0.12 Å longer for trigonal copper than for digonal copper. The limit of resolution for unfiltered EXAFS data is approximately  $\Delta R = \pi/2k$ , where  $k$  refers to the  $k$ -range fitted, and a resolution limit of 0.13 Å is obtained for separating two discrete Cu-S shells using the  $\text{Cu}_5\text{S}_6$  data set ( $\Delta R = 0.11 \text{ \AA}$  for the other two model data sets). The trigonal Cu-S bond distance additionally shows a degree of scatter around the mean distance. Because of these considerations we do not expect to be able to resolve the Cu-S EXAFS into two discrete Cu-S interactions, and this interaction is best treated as a single shell averaged over the digonal and trigonal Cu(I) contributions.

The average coordination number for the Cu-S shell can be calculated as  $N = 3x_t + 2x_d$ , where  $x_t$  and  $x_d$  are the fractions of Cu(I) ions in the cluster present in trigonal and digonal coordination, respectively. In the curve-fitting analysis bond lengths and Debye-Waller factors were floated, and the coordination values fixed at the calculated values. The results of the

curve-fitting analyses for all three compounds are summarized in Table I. The mean interatomic distances ( $r_{cryst}$ ) calculated from the crystal structures are also given in Table I. There is an excellent correspondence between the two techniques, with agreement in interatomic distance to better than 0.01 Å for all shells, with the sole exception of the small outer Cu-Cu shell for  $Cu_5S_6$ , which differs by -0.07 Å. The value of  $\sigma_{stat}^2$ , the static contribution to the Debye-Waller factor, is calculated from the distribution of bond distances in the crystal structure [cf. 38]. We observe a correlation between  $\sigma_{stat}^2$  and the total Debye-Waller factor,  $\sigma_{total}^2$ , obtained from the EXAFS curve-fitting analysis, with both values increasing with increased disorder of the interatomic distances. We calculate that a maximum  $\sigma_{stat}^2$  is expected for fraction of digonal Cu(I) in the cluster of 0.6, because for this value there are equal numbers of trigonal and digonal Cu-S bonds. If it is assumed that  $\sigma_{total}^2 = \sigma_{stat}^2 + \sigma_{vib}^2$ , where  $\sigma_{vib}^2$  is the vibrational contribution to the Debye-Waller factor, then values of 0.0036, 0.0035 and 0.0031 Å<sup>2</sup> for  $\sigma_{vib}^2$  are calculated for  $x_d = 0.0, 0.2$  and  $0.6$ , respectively. These values fall within the chemically expected range, and follow the expected trend towards smaller values for shorter bond lengths. As Debye-Waller factors are notoriously difficult to quantify, the observed trend and the chemical sensibility of these values is most gratifying.

The mean Cu-S bond distances deduced from the EXAFS analysis for the model cluster compounds show a systematic decrease with the fraction of digonal copper. Figure 4 shows these values for the three compounds, together with a predictive curve of the form:

$$R_{av} = \frac{2x_d R_d + 3x_t R_t}{2x_d + 3x_t}$$

where  $x_d, x_t$  are the fractions of digonal and trigonal copper, respectively, and  $R_d$  and  $R_t$  are the corresponding Cu-S bond distances for exclusive digonal and trigonal coordination. The curve thus predicts the mean Cu-S bond distances, weighted appropriately. From a consideration of a variety of synthetic copper(I)-thiolate cluster crystal structure data with different thiolate ligands, values of 2.16 and 2.28 Å were chosen for  $R_d$  and  $R_t$ , respectively. It can be seen that excellent correlation is obtained between the observed bond distances and the curve. Thus, one may conclude that the mean Cu-S distance obtained from EXAFS may be used to measure the fraction of digonal copper in biological cuprous-thiolate clusters.

*Cu K-edge XAS of copper(I)-thiolate clusters in metalloproteins.* The data reported in this work are comprised of a re-analysis of some previously published data, with new data on three different proteins; *S. cerevisiae* copper metallothionein, *S. pombe* Cu-( $\gamma$ EC)<sub>n</sub>G complex, and, of particular note, CuE7, an oncogenic DNA binding protein from *Papilloma* virus. The edge spectra the different metalloproteins are compared in Figure 5. It can be seen that all the spectra are very similar; all have a pronounced feature at about 8984 eV, and all show a strong similarity to the model compound copper-thiolate cluster spectra shown in Figure 2.

Cu K-edge EXAFS spectra of metalloprotein samples are shown in Figure 6 and the corresponding Fourier transforms in Figure 7. The Fourier transforms have a similar form to those of the synthetic cluster compounds (Figure 3B). Each of the Fourier transforms shows a prominent first-shell Cu-S contact, and all samples additionally show a second, smaller contact which corresponds to the Cu-Cu shell. The presence of the Cu-Cu contact is indicative of the presence of a copper-thiolate cluster in these proteins.

EXAFS curve-fitting analysis was carried out on the metalloprotein samples. In these cases, the average coordination numbers for the copper centers are not known. An independent determination of average coordination number for an unknown cluster from EXAFS data is difficult, since there is a very high correlation (generally > 90%) between  $N$  and  $\sigma^2$  for a particular shell. In order to estimate a coordination number for the Cu-S shell, the value of the coordination number was incremented in steps of 0.2, and a fit was carried out at each step with  $R$  and  $\sigma^2$  of all shells floating. The coordination number corresponding to the best fit was then chosen and held constant. The estimates of coordination numbers thus obtained for the Cu-S shell lie in the range  $2.6 \leq N \leq 3.0$ , which, by analogy with the synthetic model clusters, are plausible. The corresponding Debye-Waller factors lie in the range  $0.0038 \leq \sigma^2 \leq 0.0057 \text{ \AA}^2$ , which again compare well with the values for the model compounds. The value of  $N$  for the Cu-Cu shells was chosen in a similar way, applying an increment of 0.5 in  $N$ . In each case the presence of two Cu-Cu shells, the first at around 2.7 Å and the second at 3.0-3.2 Å was tested, but only in the case of the CuE7 protein from the *Papilloma* virus was a significant improvement in the fit obtained by the addition of an extra shell. In the case of *S. cerevisiae* copper metallothionein (I), an additional Cu-Cu shell at 4.02 Å was added, significantly improving the fit. The results of the EXAFS curve-fitting are given in Table II.

The predictive curve of Figure 4 was then used to estimate the fraction of digonally

coordinated Cu(I) present in the cuprous-thiolate metalloprotein clusters, using the mean Cu-S distance as obtained from EXAFS curve-fitting analysis. The results are shown in Table III, and include analysis of new data, together with some re-analysis of previously published EXAFS data [2,39], using the same phase and amplitude functions used in the EXAFS analysis of the model compounds (see experimental section). Also included are the predictions for two proteins from other workers [40,41]; however as these values were obtained using different phase and amplitude functions compared with those used to generate Figure 4, the estimate of the fraction of digonal Cu(I) may be less reliable. The values for  $x_d$  shown in Table III vary from 0.1 (*i.e.* close to pure trigonal copper) to 0.5.

## Discussion

We have previously reported copper K-edge and sulfur K-edge EXAFS analyses of copper metallothionein from *S. cerevisiae* [2]. The Cu-S distances determined for the wild-type metallothionein, and two truncated mutant proteins were all close to 2.24 Å [2]. Re-analysis of the original wild-type EXAFS data by curve fitting using the current, much improved, phase and amplitude functions yielded a best fit with a mean Cu-S distance of 2.242 Å, and a mean coordination number of 2.6 (see Table II, sample (I)), in excellent agreement with the original analysis. We also collected new EXAFS data on a second yeast copper metallothionein isolate (Table II), although in this case trace zinc contamination limited the maximum  $k$  to 13 Å<sup>-1</sup>. A marginally longer mean Cu-S distance of 2.250 Å was obtained with this new data set. A comparison of these mean Cu-S distances to the results of the synthetic cuprous-thiolate clusters in Figure 4 predicts a fraction of digonal Cu(I) ions in *S. cerevisiae* copper metallothionein of 0.3-0.4 (see Table III). This value is consistent with the likely fraction of digonal Ag(I) of 2/7 determined by HMQC NMR measurements of silver metallothionein [3]. For both data sets, a well-defined second shell of Cu-Cu contacts was indicative of the presence of a multimetallic cuprous-thiolate cluster.

X-ray absorption studies were performed on *in vivo* produced Cu-( $\gamma$ EC)<sub>*n*</sub>G peptide complexes from *S. pombe*, and synthetically produced Cu-( $\alpha$ EC)<sub>*n*</sub>G and Cu-( $\gamma$ EC)<sub>*n*</sub>G complexes. The isopeptides, (Glu-Cys)<sub>*n*</sub>Gly, differ from glutathione in having multiple (Glu-Cys) dipeptide units with 2 ≤ *n* ≤ 6 [5]. The complexes are oligomers of undefined M<sub>*r*</sub>, so that the

precise Cu(I) stoichiometry is uncertain, although 4-6 Cu(I) per complex seem likely [5]. Mean Cu-S bond distances of 2.270, 2.278, and 2.257 Å were determined by EXAFS curve-fitting for *S. pombe* Cu-( $\gamma$ EC)<sub>n</sub>G, synthetic Cu-( $\gamma$ EC)<sub>n</sub>G and synthetic Cu-( $\alpha$ EC)<sub>n</sub>G, respectively. Using the correlation of Figure 4, these distances indicate a close to exclusive trigonal coordination of the Cu(I) by sulfur in the Cu-( $\gamma$ EC)<sub>n</sub>G complexes, but a significant fraction of digonal copper (0.3) in the case of the Cu-( $\alpha$ EC)<sub>n</sub>G complex. For the Cu-( $\gamma$ EC)<sub>n</sub>G complexes, clearly defined Cu-Cu interactions, apparent in the outer shell at 2.75 Å, indicate multimetallic copper-thiolate clusters. The EXAFS of the native and synthetic Cu-( $\gamma$ EC)<sub>n</sub>G complexes, were found to be quite similar, although the curve fitting gave a larger *N* for the Cu-Cu interaction in the synthetic complex. We were not able to observe a Cu-Cu interaction in the Cu-( $\alpha$ EC)<sub>n</sub>G EXAFS. Nevertheless, the presence of a cluster seems highly probable [5]. It seems possible that the slightly lower signal to noise ratio of this data, perhaps combined with some heterogeneity in Cu-Cu distances, makes the Cu-Cu interaction unobservable in this case.

In previous work, we have reported Cu K-edge X-ray absorption studies on the N-terminal half of the ACE1 polypeptide as a Cu(I) complex, both as CuACE1 samples purified from a bacterial expression system, and as CuACE1 prepared by *in vitro* reconstitution protocols from the apo-protein [9,10]. The CuS cluster in CuACE1 contains 6-7 copper atoms [9]. The edge spectrum of CuACE1 was observed to be dominated by an edge feature near 8983 eV, very similar to that seen in copper metallothionein. Based in part on the model compound data of Kau *et al.* [36], the conclusion was reached that the Cu(I) ions were predominantly trigonal [9,10]. New data have been recorded for a CuACE1 prepared by *in vitro* reconstitution using Cu : glutathione as the Cu(I) donor (Figure 5-7). Curve-fitting analysis of the EXAFS of CuACE1 (Figure 7, Table II) reveals a mean Cu-S bond distance of 2.258 Å, which is very similar to that found in our previous work [9,10] (Table II). The correlation in Figure 4 suggests that the stoichiometry of CuACE1 may be represented by 1-2 digonal and 4-5 trigonal Cu(I) ions. As with metallothionein the presence of a cluster in CuACE1 is indicated by the Cu-Cu interactions apparent in the EXAFS, which, at 2.72 Å, are similar to the short Cu-Cu distances observed in copper metallothioneins and synthetic trigonally coordinated copper-thiolate clusters. The Cu-Cu outer shell is much better defined in the present CuACE1 data than for both ACE1 prepared by reconstitution in the absence of glutathione [9], and for native yeast copper metallothionein.

The E7 protein from *papilloma* viruses is a metalloprotein. The identity of the metal ion populating the binding site in virally infected cells is unclear, but expression of E7 genes from human HPV16 *papilloma* and rabbit *papilloma* viruses in an *E. coli* expression system yields E7 protein as a ZnE7 protein complex [15,16]. The Zn(II) ions in the E7 proteins undergo a rapid metal exchange reaction with Cu(I) ions yielding CuE7 proteins with stoichiometries of 2 and 3 mol eq. for HPV16 and rabbit *papilloma* virus CuE7s, respectively [15]. X-ray absorption spectroscopy on rabbit *papilloma* virus CuE7 revealed a mean Cu-S distance of 2.265 Å and the presence of a Cu-Cu scatter peak indicative of a multimetallic CuS cluster. As CuE7 contains only 3 mol eq. Cu(I), any digonally coordinated Cu(I) ions would be expected to be more clearly evident in the mean Cu-S distance compared to copper-thiolate clusters of higher nuclearity. Data are most consistent with exclusively trigonal Cu(I) coordination.

## Conclusion

The identification of the coordination geometry within a given cuprous-thiolate multimetallic cluster is a difficult problem. The Cu K-edge X-ray absorption data, together with careful analysis of Cu-S bond distances from EXAFS appear to be the best spectroscopic indicator in the absence of other structural data. From the Cu(I)-thiolate synthetic model compounds discussed here, it appears that the mean Cu-S bond distance is a significantly better indicator than the nature of the 8983 eV edge feature in the edge spectrum.

## Acknowledgements

We thank Professor Keith Hodgson for the *Neurospora crassa* metallothionein EXAFS data, and also for helpful discussion. We are indebted to the staff of the Stanford Synchrotron Radiation Laboratory (SSRL) for their assistance. SSRL is funded by the Department of Energy (Office of Basic Energy Sciences, Division of Chemical Sciences, and Office of Health and Environmental Resources) and the National Institutes of Health (Biotechnology Resource Program, Division of Research Resources). We also thank Dr. Garry S. H. Lee for preparation of model compounds. D.R.W. is supported by the National Institutes of Health (ES 03817). C.T.D. is supported by Training Grant T32 AM 07115 from the National Institutes of Health.

## References

1. Winge, D. R.; Dameron, C. T.; George, G. N. *Adv. in Inorg. Biochem.* **1993**, *10* (in press).
2. (a) George, G. N.; Byrd, J.; Winge, D. R. *J. Biol. Chem.* **1988**, *263*, 8199-8203.  
(b) George, G. N.; Winge, D. R.; Stout, C. D.; Cramer, S. P. *J. Inorg. Biochem.* **1986**, *27*, 213-220.
3. Narula, S. S.; Mehra, R. K.; Winge, D. R.; Armitage, I. M. *J. Am. Chem. Soc.* **1991**, *113*, 9354-9358.
4. (a) Hamer, D.H.; Thiele, D.J.; Lemontt, L.E. *Science* **1985**, *228*, 685-690.  
(b) Wright, C.F.; Hamer, D.H.; McKenney, K. *J. Biol. Chem.* **1968**, *263*, 1570-1574  
(c) Ecker, D.J.; Butt, T.R.; Sternberg, E.J.; Neeper, M.P.; Debouck, C.; Gorman, J.A.; Crooke, S.T. *J. Biol. Chem.* **1986**, *261*, 16895-16900.
5. Reese, R.N.; Mehra, R. K.; Tarbet, E. B.; Winge, D. R. *J. Biol. Chem.* **1988**, *263*, 4186-4192.
6. Hamer, D. H. *Annual Rev. Biochem.* **1986**, *55*, 913-951.
7. Bremner, I. *Experientia Suppl.* **1987**, *52*, 81-104.
8. (a) Furst, P.; Hu, S.; Hackett, R.; Hamer, D. H. *Cell* **1988**, *55*, 705-717.  
(b) Thiele, D. J. *Mol. Cell. Biol.* **1988**, *8*, 2745-2752.
9. Dameron, C. T.; Winge, D. R.; George, G. N.; Sansone, M.; Hu, S.; Hamer, D. *Proc. Natl. Acad. Sci. USA* **1991**, *88*, 6127-6131.
10. Nakagawa, K.H.; Inouye, C.; Hedman, B.; Karin, M.; Tullius, T.D.; Hodgson, K.O. *J. Am. Chem. Soc.* **1991**, *113*, 3621-3623.
11. Zhou, P.; Thiele, D. J. *Proc. Natl. Acad. Sci. USA* **1991**, *88*, 6112-6116.
12. Thiele, D. J. *Nuc. Acid Res.* **1992**, *20*, 1183-1191.
13. Welch, J.; Fogel, S.; Buchman, C.; Karin, M. *EMBO J.* **1989**, *8*, 255-260.
14. Hu, S.; Furst, P.; Hamer, D. *New Biologist* **1990**, *2*, 544-555.
15. Zhou, P.; Szczyepka, M.S.; Sosinowski, T.; Thiele, D.J. *Mol. Cell. Biol.* **1992**, *12*, 3766-3775.

16. Roth, E. J.; Kurz, B.; Liang, L.; Hansen, C. L.; Dameron, C. T.; Winge, D. R.; Smotkin, D. *J. Biol. Chem.* **1992**, *267*, 16390-16395.
17. (a) Uchida, Y.; Takio, K.; Titani, K.; Ihara, Y.; Tomonaga, M. *Neuron* **1991** *7*, 337-347.  
(b) Palmiter, R. D.; Findley, S. D.; Whitmore, T. E.; Dumam, D. M. *Proc. Natl. Acad. Sci. USA* **1992**, *89*, 6333-6337.
18. Kagi, J. H. R.; Schaffer, A. *Biochemistry* **1988**, *27*, 8509-8515.
19. Winge, D. R.; Nielson, K. B.; Gray, W. R.; Hamer, D. H. *J. Biol. Chem.* **1985**, *260*, 14464-14470.
20. Dance, I. G. *Polyhedron* **1986**, *5*, 1037-1104.
21. Dance, I. G.; Calabrese, J. C. *Inorg. Chim. Acta* **1976**, *19*, L41-L42.
22. Coucouvanis, D.; Murphy, C. N.; Kanodia, S. K. *Inorg. Chem.* **1980**, *19*, 2993-2998.
23. Dance, I. G.; Bowmaker, G. A.; Clark, G. R.; Seadon, J. K. *Polyhedron* **1983**, *2*, 1031-1043.
24. Nicholson, J. R.; Abrahams, I. L.; Clegg, W.; Garner, C. D. *Inorg. Chem.* **1985**, *24*, 1092-1096.
25. Bowmaker, G. A.; Clark, G. R.; Seadon, F. J. K.; Dance, I. G. *Polyhedron* **1984**, *3*, 535-544.
26. Dance, I. G. *Aust. J. Chem.* **1978**, *31*, 2195-2206.
27. Hollander, F. J.; Coucouvanis, D. *J. Am. Chem. Soc.* **1974**, *96*, 5646-5648.
28. Birker, P. J. M. L.; Freeman, H. C. *J. Am. Chem. Soc.* **1977**, *99*, 6890-6899.
29. (a) Dance, I.; Fischer, K.; Lee, G.; chapter 13, in *Metallothioneins, Synthesis, Structure and Properties of Metallothioneins, Phytochelatins and Metal Thiolate Complexes*, eds. Stillman, M.J.; Shaw III, C.F.; Suzuki, K.T.; VCH New York **1992**.  
(b) Tang, K.; Tang, Y. chapter 20, in *Heteroatom Chemistry*, ed. Block, E. VCH New York, **1990**.



- (c) Tang, Q.; Tang, K.; Liao, H.; Han, Y.; Chen, Z.; Tang, Y. *J. Chem. Soc., Chem. Commun.* **1987**, 1076- ?.
30. Throughout this paper S refers to cysteinyl or thiolate sulfur.
31. Bowmaker, G.A.; Tan, L-C. *Aust. J. Chem.* **1979**, *32*, 1443-1452.
32. Cramer, S.P.; Tench, O.; Yocum, M.; George, G.N. *Nucl. Instrum. Methods. Phys. Res.* **1988** *A266*, 586-591.
33. George, G. N.; Kipke, C. A.; Prince, R. C.; Sunde, R. A.; Enemark, J. H.; Cramer, S. P. *Biochemistry* **1989**, *28*, 5075-5080.
34. (a) Rehr, J. J.; Mustre de Leon, J.; Zabinsky, S. I.; Albers, R. C. *J. Am. Chem. Soc.* **1991**, *113*, 5135-5140.
- (b) Mustre de Leon, J.; Rehr, J. J.; Zabinsky, S. I. *Phys. Rev. B.* **1991**, *44*, 4146-4156.
35. Weininger, M.S.; Hunt, G.W.; Amma, E.L. *J. Chem. Soc., Chem. Commun.* **1972**, 1140-1141.
36. Kau, L. S.; Spira-Solomon, D. J.; Penner-Hahn, J. E.; Hodgson, K. O.; Solomon, E. I. *J. Am. Chem. Soc.* **1987**, *109*, 6433-6442.
37. Dance, I.G. *J. Chem. Soc., Chem. Commun.* **1976**, 68-69.
38. e.g. See: Teo, B.K. in *EXAFS: Basic Principles and Data Analysis*, Springer-Verlag, Berlin, Heidelberg, New York, Tokyo, **1986**.
39. Smith, T. A.; Lerch, K.; Hodgson, K. O. *Inorg. Chem.* **1986**, *25*, 4677-4680.
40. Abrahams, I.L.; Bremner, I.; Diakun, G.P.; Garner, C.D.; Hasnain, S.S.; Ross, I.; Vasak, M. *Biochem. J.* **1986**, *236*, 585-589.
41. Freedman, J.H.; Powers, L.; Peisach, J. *Biochemistry* **1986**, *25*, 2342-2349.

**Table I.** Results of Cu K-Edge EXAFS Curve-Fitting of Copper(I)-Thiolate Cluster Model Compounds.

		$\text{Cu}_4\text{S}_6$	$\text{Cu}_5\text{S}_7$	$\text{Cu}_5\text{S}_6$
Fraction of digonal Cu, $x_{dig}$		0	0.2	0.6
Range in $k$ refined ( $\text{\AA}^{-1}$ )		1-15	1-15	1-13
Cu-S	$N$	3	2.8	2.4
	$R$ ( $\text{\AA}$ )	2.282(2)	2.258(2)	2.229(3)
	$\sigma^2$ ( $\text{\AA}^2$ )	0.0045(2)	0.0055(2)	0.0065(4)
	$r_{cryst}$ ( $\text{\AA}$ ) <sup>a</sup>	2.291	2.254	2.221
	$\sigma_{stat}^2$ ( $\text{\AA}^2$ ) <sup>b</sup>	0.0009	0.0020	0.0034
Cu-Cu	$N$	3 <sup>d</sup>	0.8	2.4
	$R$ ( $\text{\AA}$ )	2.741(3) <sup>d</sup>	2.696(6)	2.725(3)
	$\sigma^2$ ( $\text{\AA}^2$ )	0.0075(3) <sup>d</sup>	0.0050(6)	0.0067(3)
	$r_{cryst}$ ( $\text{\AA}$ ) <sup>a</sup>	2.738	2.682	2.721
	$\sigma_{stat}^2$ ( $\text{\AA}^2$ ) <sup>b</sup>	0.0019	0.0012	0.0003
Cu-Cu	$N$	-	2	1.2
	$R$ ( $\text{\AA}$ )	-	3.025(14)	3.16(2)
	$\sigma^2$ ( $\text{\AA}^2$ )	-	0.014(2)	0.012(3)
	$r_{cryst}$ ( $\text{\AA}$ ) <sup>a</sup>	-	3.012	3.232
	$\sigma_{stat}^2$ ( $\text{\AA}^2$ ) <sup>b</sup>	-	0.0057	0.0021
$F_{fit}^c$		0.123	0.129	0.153

Notes: Values in parentheses are the 95% confidence limits, estimated as three times the estimated standard deviations obtained from the diagonal elements of the covariance matrix. These indicate the precision (as opposed to accuracy) to which parameters are determined within the constraints of the model. The presence of systematic errors (sometimes called statistical bias) will give a poorer accuracy, with major contributions from lack of transferrability of phase and amplitude functions. Typical worst-case accuracies are  $\pm 0.02\text{\AA}$  for  $R$  (with directly coordinated atoms), and  $\pm 25\%$  for  $N$  and  $\sigma^2$ . <sup>a</sup>Values of  $r_{cryst}$  are the mean bond distance calculated from

the respective crystal structures. <sup>b</sup> $\sigma_{stat}^2$  is the static contribution to the Debye-Waller factor ( $\sigma_{tot}^2 = \sigma_{vib}^2 + \sigma_{stat}^2$ ), and is calculated from the crystal structure, using  $\sigma_{stat}^2 = (\sum(r_i - r_0)^2)/n$ , where  $n$  is the number of bonds, the sum is over each bond distance  $r_i$ , and  $r_0$  is the mean bond distance. <sup>c</sup>Goodness of fit parameter, defined as  $F_{fit} = (\sum(\chi_i - \chi_0)^2 k^6)/(n_{obs} - n_{var})$  where  $\chi_i$ ,  $\chi_0$  are the observed and calculated EXAFS, respectively, and  $n_{obs}$  and  $n_{var}$  are the numbers of observations and variables, respectively. <sup>d</sup>Phase and amplitude functions for the Cu-Cu contacts calculated from this shell (see experimental section).

**Table II.** Results of Cu K-Edge EXAFS Curve-Fitting of Metalloproteins.

Metalloprotein	Interaction	$N$	$R$ (Å)	$\sigma^2$ (Å <sup>2</sup> )	$k_{max}$	$F_{fit}^a$
<i>S. cerevisiae</i> CuMT	Cu-S	2.8	2.250(4)	0.0056(5)	13.0	0.368
	Cu-Cu	0.5	2.703(11)	0.0028(10)		
<i>S. pombe</i> Cu-( $\gamma$ EC) <sub>n</sub> G	Cu-S	3.0	2.270(3)	0.0041(4)	12.8	0.487
	Cu-Cu	1.5	2.747(8)	0.0059(8)		
Synthetic Cu-( $\gamma$ EC) <sub>n</sub> G	Cu-S	3.0	2.278(3)	0.0034(3)	13.0	0.471
	Cu-Cu	2.5	2.768(10)	0.0101(11)		
Synthetic Cu-( $\alpha$ EC) <sub>n</sub> G	Cu-S	2.8	2.257(5)	0.0042(6)	13.0	1.05
CuACE1	Cu-S	2.8	2.258(4)	0.0043(4)	12.8	0.533
	Cu-Cu	3.0	2.717(15)	0.014(2)		
<i>Papilloma virus</i> CuE7	Cu-S	2.8	2.263(3)	0.0038(3)	12.8	0.402
	Cu-Cu	2.0	2.72(2)	0.014(3)		
	Cu-Cu	0.5	3.07(4)	0.008(5)		

Notes: <sup>a</sup>Goodness of fit parameter, defined as  $F_{fit} = (\sum(\chi_i - \chi_0)^2 k^6) / (n_{obs} - n_{var})$  where  $\chi_i, \chi_0$  are the observed and calculated EXAFS, respectively, and  $n_{obs}$  and  $n_{var}$  are the numbers of observations and variables, respectively.

**Table III.** Fractions of digonal Cu(I) in copper-thiolate clusters of metalloproteins

Metalloprotein	$R$ (Å)	Predicted $x_d$
<i>S. cerevisiae</i> CuMT [2a]	2.242 <sup>a</sup>	0.4
<i>S. cerevisiae</i> CuMT	2.250	0.3
<i>N. crassa</i> CuMT [39]	2.233 <sup>a</sup>	0.5
Rat CuMT- $\beta$ [2b]	2.255 <sup>a</sup>	0.3
Pig CuMT [40]	2.25 <sup>b</sup>	0.3
Dog CuMT [41]	2.27 <sup>b</sup>	0.1
<i>S. pombe</i> Cu-( $\gamma$ EC) <sub><i>n</i></sub> G	2.270	0.1
Synthetic Cu-( $\gamma$ EC) <sub><i>n</i></sub> G	2.278	0.0
Synthetic Cu-( $\alpha$ EC) <sub><i>n</i></sub> G	2.257	0.3
CuACE1	2.258	0.3
<i>Papilloma virus</i> CuE7	2.263	0.2

Notes: *a.* EXAFS data for these proteins has been reevaluated using the same phase and amplitude functions as employed in this work. *b.* Values of  $R$  for these proteins have been taken from the literature, in this case the systematic difference between the EXAFS phase and amplitudes means that the estimated value for  $x_d$  must be considered less accurate.

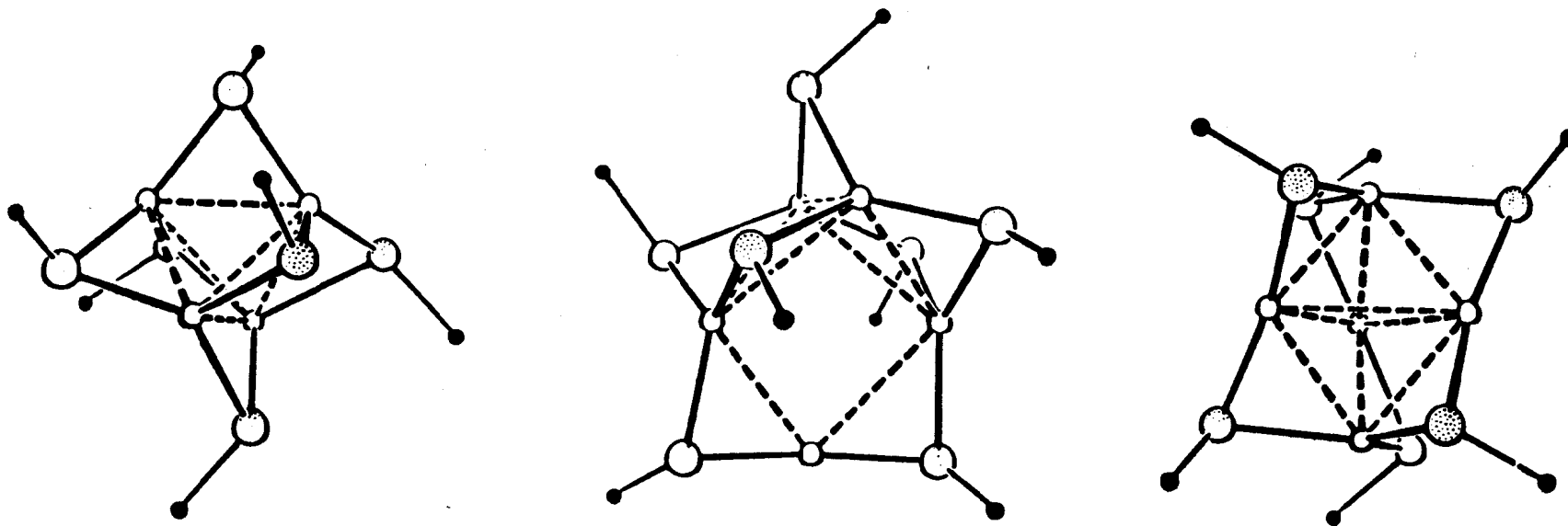


Figure 1

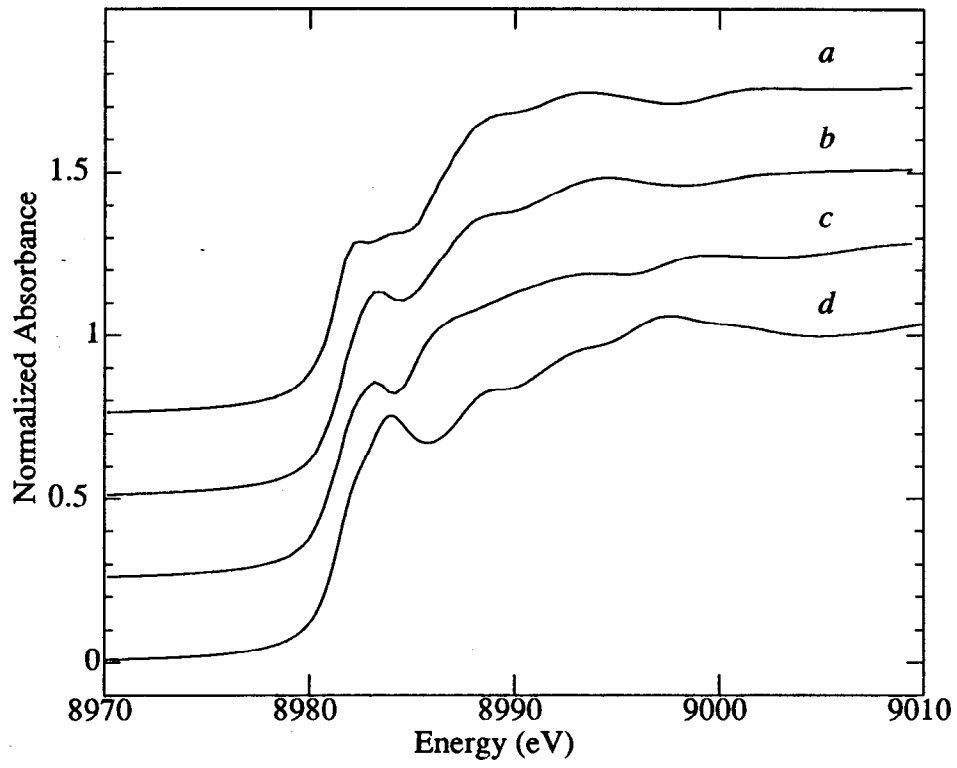


Figure 2

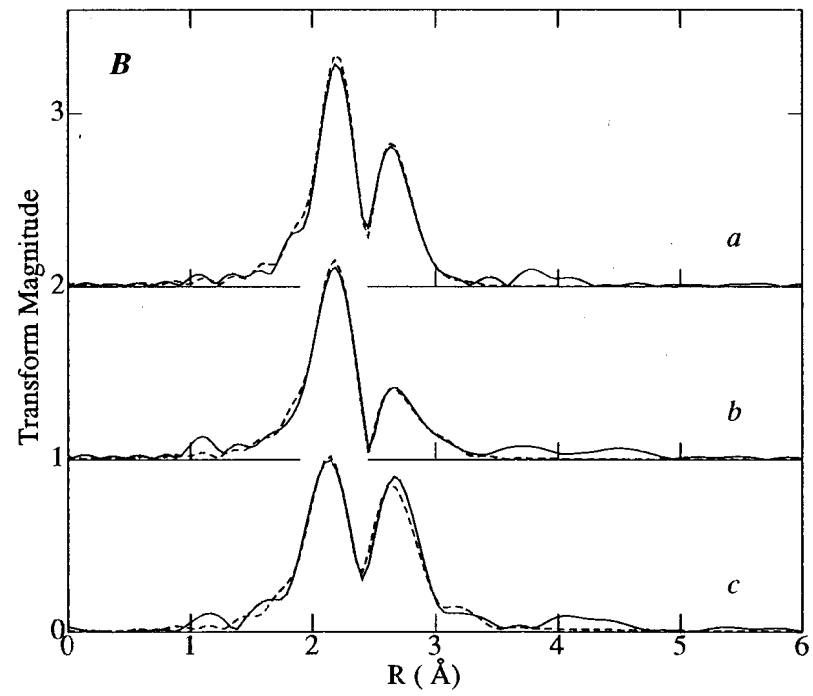
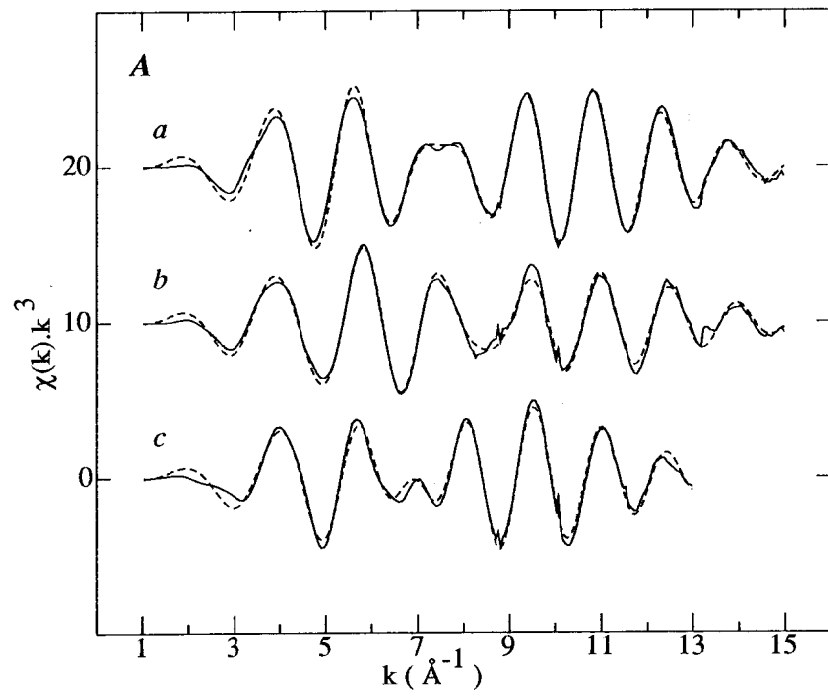


Figure 3



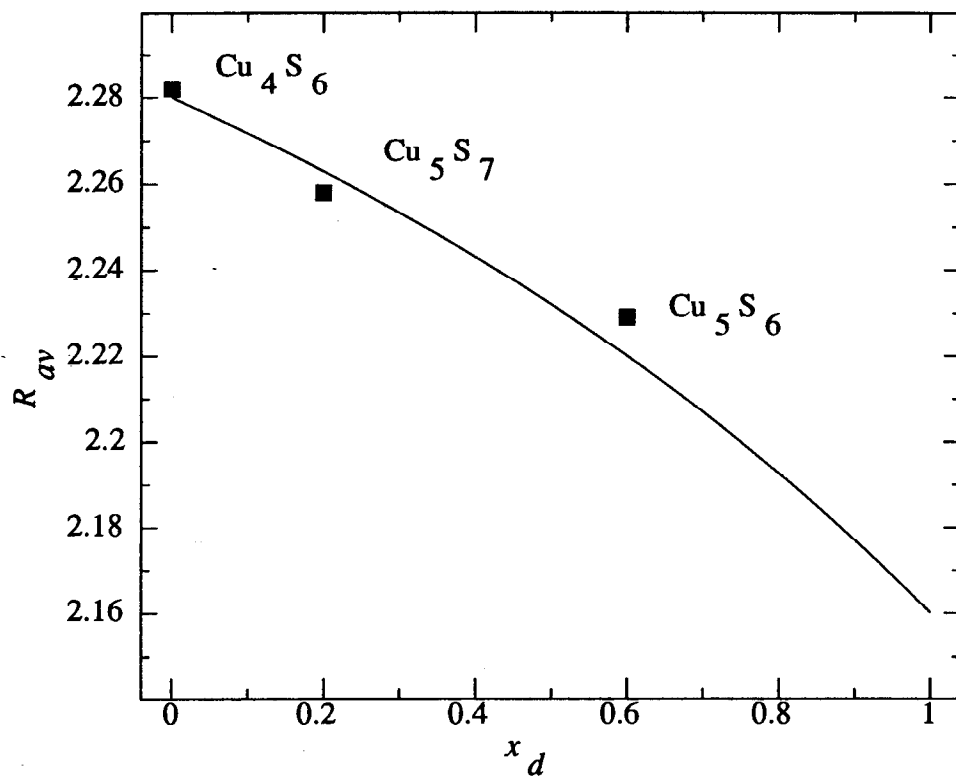


Figure 4

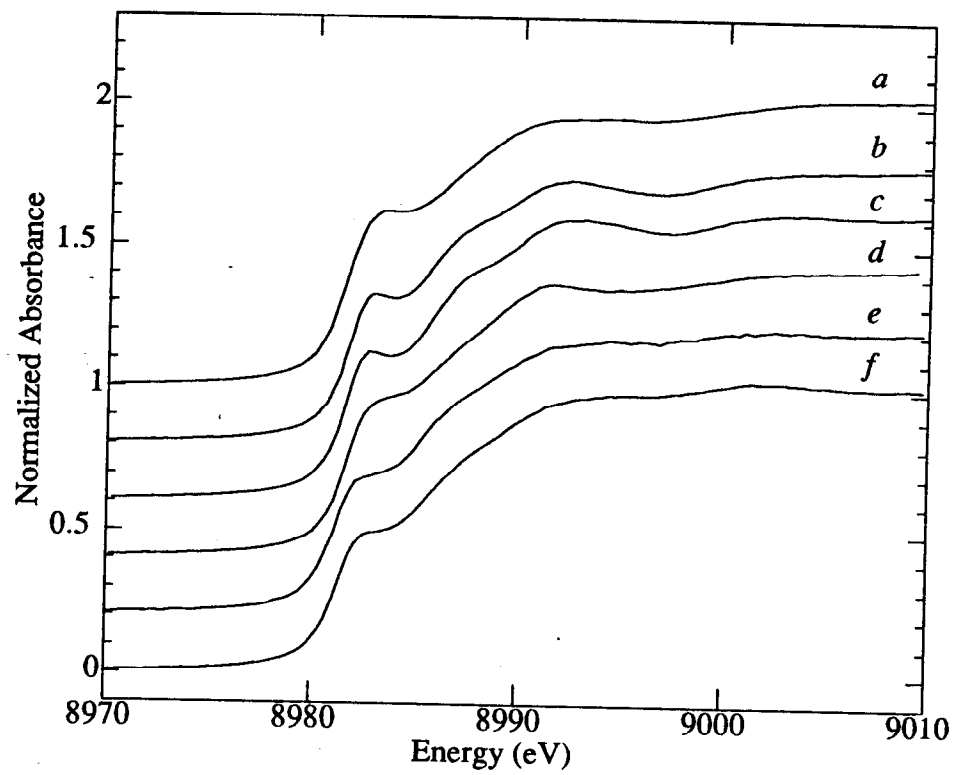


Figure 5

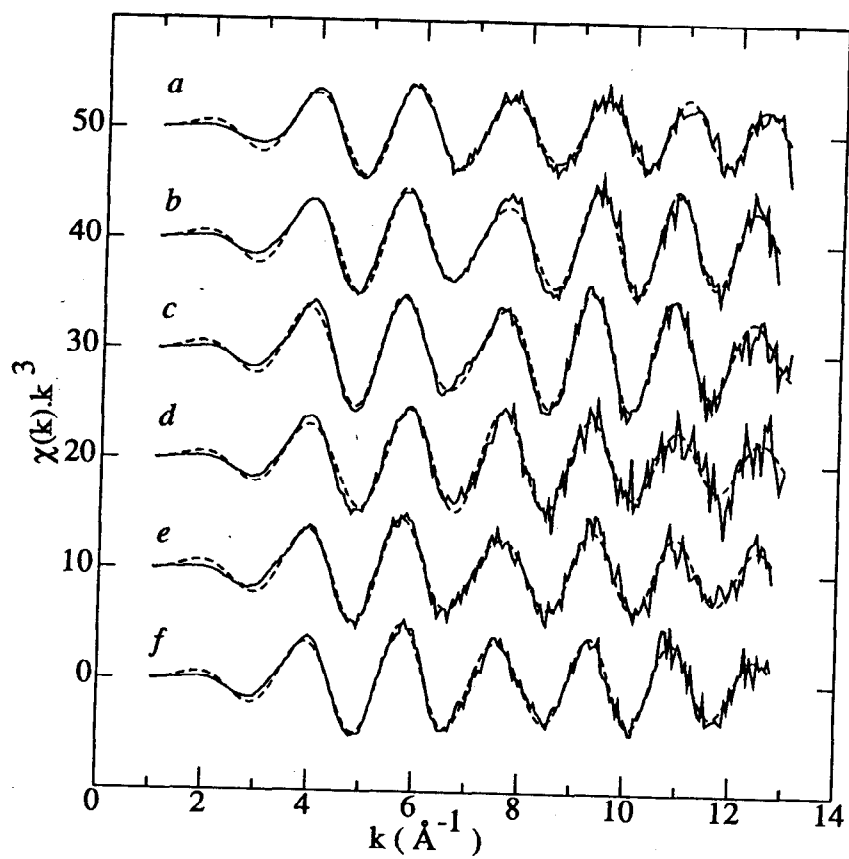


Figure 6

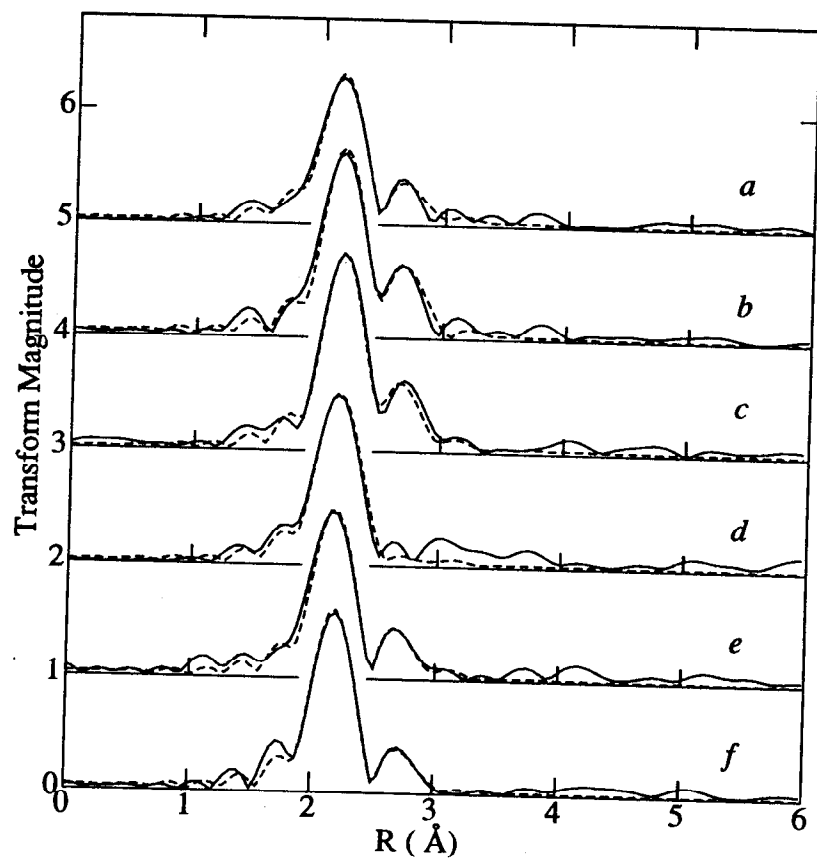


Figure 7